TEC-0109

Extraction of Micro-Terrain Features

William B. Thompson

University of Utah - Computer Science
50 S. Central Campus Drive
Salt Lake City, UT 84112-9205

Evans and Sutherland Corporation
600 Komas Drive
Salt Lake City, UT 84108

August 1998

19980826 010

Approved for public release; distribution is unlimited.

Prepared for:
Defense Advanced Research Projects Agency
3701 North Fairfax Drive
Arlington, VA 22203-1714

DTIC QUALITY INSPECTED 1

Monitored by:
U.S. Army Corps of Engineers
Topographic Engineering Center
7701 Telegraph Road
Alexandria, VA 22315-3864

US Army Corps of Engineers
Topographic Engineering Center

T

E

C

Destroy this report when no longer needed.
Do not return it to the originator.

The findings in this report are not to be construed as an official Department of the Army position unless so designated by other authorized documents.

The citation in this report of trade names of commercially available products does not constitute official endorsement or approval of the use of such products.

REPORT DOCUMENTATION PAGE

Form Approved
OMB No. 0704-0188

Public reporting burden for this collection of information is estimated to average 1 hour per response, including the time for reviewing instructions, searching existing data sources, gathering and maintaining the data needed, and completing and reviewing the collection of information. Send comments regarding this burden estimate or any other aspect of this collection of information, including suggestions for reducing this burden, to Washington Headquarters Services, Directorate for Information Operations and Reports, 1215 Jefferson Davis Highway, Suite 1204, Arlington, VA 22202-4302, and to the Office of Management and Budget, Paperwork Reduction Project (0704-0188), Washington, DC 20503.

1. AGENCY USE ONLY *(Leave blank)*	2. REPORT DATE	3. REPORT TYPE AND DATES COVERED
	August 1998	Technical January 1997 - April 1998

4. TITLE AND SUBTITLE

Extraction of Micro-Terrain Features

5. FUNDING NUMBERS

DACA76-97-K-0003

6. AUTHOR(S)

William B. Thompson

7. PERFORMING ORGANIZATION NAME(S) AND ADDRESS(ES)

University of Utah - Department of Computer Science
50 S. Central Campus Drive, Room 3190
Salt Lake City, UT 84112-9205
(also, see block #11, below)

8. PERFORMING ORGANIZATION REPORT NUMBER

9. SPONSORING / MONITORING AGENCY NAME(S) AND ADDRESS(ES)

Defense Advanced Research Projects Agency
3701 N. Fairfax Drive, Arlington, VA 22203

U.S. Army Topographic Engineering Center
7701 Telegraph Road, Alexandria, VA 22315-3864

19. SPONSORING / MONITORING AGENCY REPORT NUMBER

TEC-0109

11. SUPPLEMENTARY NOTES

Evans and Sutherland Corporation
600 Komas Drive
Salt Lake City, UT 84108

12a. DISTRIBUTION / AVAILABILITY STATEMENT

Approved for public release; distribution is unlimited.

12b. DISTRIBUTION CODE

13. ABSTRACT *(Maximum 200 words)*

Micro-terrain features are topographic structures relevent to the behavior of a simulation, but with a horizontal extent significantly less than the resolution of the base-level terrain data covering the area in which these structures occur. Thus, these features are not directly extractable from elevation data. While they are often apparent in aerial imagery, micro-terrain features are easily missed or confused with other features, making reliable detection, based on imagery alone, problematic. This report describes an automated method for extracting high fidelity models of small-scale ravine features by augmenting a hydrological analysis with computer vision techniques.

14. SUBJECT TERMS

Terrain Modeling, Imager Understanding, Simulation, Feature Extraction

15. NUMBER OF PAGES

29

16. PRICE CODE

17. SECURITY CLASSIFICATION OF REPORT	18. SECURITY CLASSIFICATION OF THIS PAGE	19. SECURITY CLASSIFICATION OF ABSTRACT	20. LIMITATION OF ABSTRACT
UNCLASSIFIED	UNCLASSIFIED	UNCLASSIFIED	UNLIMITED

TABLE OF CONTENTS

1 Overview 1

2 Introduction 1

3 Approach 2

4 Background 3

4.1 Hydrological Analysis for Terrain Analysis 3

4.2 Active Contours for Image Analysis 3

5 Ravine Extraction 4

5.1 Finding Drainage Features 4

5.2 Refining Drainage Features Using Aerial Imagery 6

5.3 Comparison with Other Analyses of Range 400 12

6 Determine the Width of Ravines 16

7 Using Active Contours to Refine Existing Features 21

LIST OF FIGURES

1 Shallow wash located within Range 400. 2

2 Combining terrain analysis and computer vision for ravine extraction. 3

3 Overview of ravine extraction process. 4

4 ITD drainage features in a portion of Range 400. 5

5 Drainage features for the same regions as shown in Figure 4, determined using hydrological analysis. 5

6 Aerial image. 7

7 Edges derived from Figure 6. 7

8 Potential function derived from edges shown in Figure 7. 8

9 Final features. 8

10 Final features, overlayed onto aerial image. 9

11 Final features, overlayed onto shaded relief generated from 1m elevation data. 9

12 Final features – full Range 400, overlayed onto shaded relief. 10

13 CCTT database with ITD-based drainage features. 11

14 CCTT database with improved ravine features. 11

15 Location of sections of Range 400 that were deemed by Richbourg as untraversable by armor are shown in black. 13

16 Marked in black are the routes determined by Richbourg from analysis of the high-quality 1m elevation data to be minimum visibility approaches to the defensive positions (marked by black ellipses). 14

17 Marked in black are the locations of washes as determined by analysis of 30m elevation data and 1m orthoimage. 15

18 Aerial image. 17

19 Potential function. 17

20 Gradient of potential function. 18

21 Extracted ravine sides. 18

22 Extracted ravine sides, overlayed onto aerial image. 19

23 Extracted ravine sides, overlayed onto shaded relief. 19

24 Extracted ravine sides – full Range 400, overlayed onto shaded relief. 20

25 Extracted ravine sides rendered onto high-resolution DEM. 21

26 ITD drainage feature. 22

27 Refined ITD drainage feature. 22

Preface

This research was supported by the Defense Advanced Research Projects Agency (DARPA) and was monitored by the U.S. Toographic Engineering Center (TEC) under contract No. DACA76-97-K-0003. The DARPA Program Manager is Mr. George Lukes and the TEC Contracting Officer's Representatvie is Ms. Lauretta Williams.

Extraction of Micro-Terrain Features

1 Overview

Micro-terrain features are topographic structures relevant to the behavior of a simulation but with a horizontal extent significantly less than the resolution of the base-level terrain data covering the area in which these structures occur. Thus these features are not directly extractable from elevation data. While they are often apparent in aerial imagery, micro-terrain features are easily missed or confused with other features, making reliable detection, based on imagery, alone problematic.

This report describes an automated method for extracting high fidelity models of small-scale ravine features by augmenting a hydrological analysis with computer vision techniques. The method extracts such features from a combined analysis of medium resolution ($\sim$ 30m) elevation data and high resolution ($\sim$ 1m GSD) monoscopic imagery. The method is tested on data covering the Range 400 live fire area of the USMC Air Ground Combat Center, located at Twentynine Palms, CA. This is a semi-arid environment containing V-bottomed ravines in hilly areas and shallow, steep sided dry washes in the piedmont.

2 Introduction

Sensor technology, limitations of photogrammetry, storage constraints, and requirements for real-time rendering all limit the fidelity with which terrain can be effectively represented in a geospatial database. For certain applications, it is critical that these databases include specific *micro-terrain* features with a lateral extent less than the resolution of base-level terrain description. Ravines and other similar drainage features are examples of topographic micro-terrain that can critically affect the realism of simulations [1].

While ravines and dry washes are usually at least partially visible on aerial photographs, accurate detection and localization is difficult. In addition, ravines are easily confused with roads, tracks, and other structures commonly appearing in non-urban environments. Photogrammetry fails to extract many ravine features because of their restricted depth and small width relative to the resolution with which terrain elevation is extracted. As a result, adding such features to terrain databases currently requires substantial manual processing.

The dry wash shown in Figure 1 is located in the live fire range (Range 400) of the USMC Air Ground Combat Center, located at Twentynine Palms, CA. The wash is 1m-2m deep and 2m-3m across. Though *very* small compared to the resolution at which terrain features are usually modeled, such ravines are of critical tactical significance to dismounted infantry, and therefore to all units in a combat force. This area is included within the coverage of the Army's Close Combat Tactical Trainer Southwest United States Desert Database (CCTT Primary Two) [2]. As a result, it provides an effective opportunity to investigate the utility of methods, such as those presented here, compared to current practice.

Standard NIMA (National Imagey and Mapping Agency) data product are available for this area, including DTED (Digital Terrain Elevation Data) level 1 and 2 elevation data and ITD (Interim Terrain Database) feature data. In addition, a 3.3km by 2.2km area is covered by a custom-produced high-quality DEM (digital elevation model) with a 1m post spacing and a relative vertical accuracy on the order of 0.1 to 0.3 meters

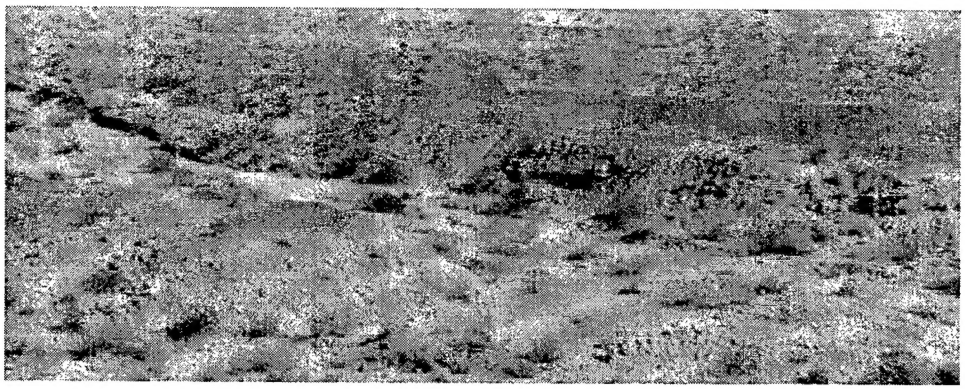

Figure 1: Shallow wash located within Range 400.

with a matching orthoimage at the same resolution [3, 4]. This provides an indication of the true topography, which we compare with estimates extracted from more commonly available data sources.

3 Approach

The nominal resolution of elevation data on which terrain models are based is commonly on the order of 30m or greater. Because of the smoothing inherent in the manner in which the elevation data is obtained, the effective resolution, measured in terms of the size of distinct features apparent in the data, is much coarser. Thus, even with DEM data finer than a 30m grid, terrain structure such as shown in Figure 1 is likely to go unrepresented. Nevertheless, coarse resolution DEMs can be used to predict likely locations where smaller terrain deformations are to be expected [5].

Ravines are erosional features generated by large-scale processes, even if the final effect is visible mostly on a fine-scale. As a result, hydrological analysis can be used to predict where such erosion is most likely to occur. Effective algorithms for performing this analysis, even on low-resolution, error-full representations of the terrain skin, are now a standard function in many geographic information systems (GIS). Such operations can be used to effectively estimate the existence and location of ravine features using DEM data with a post spacing significantly greater than the width of the features of interest.

Hydrological analysis alone is not sufficient to confirm that a ravine actually exists or to accurately determine its location. Our approach therefore uses computer vision techniques applied to higher resolution aerial images to refine the results of the hydrological processing. Figure 2 illustrates the method. The contour maps show elevations in a small patch of terrain, determined based on DTED level 2 data with a post spacing of approximately 30m. Hydrologic features are overlayed on the right-most map. The lower left shows a 1m resolution orthoimage of the same area. To its right is the results of a standard edge detector applied to this image. Neither the hydrological drainage features nor the edge features are enough in isolation to accurately locate the ravines. Taken together, however, accurate localization is possible, as shown on the far right of the figure. Here, the results of automated ravine extraction are overlayed on a shaded relief rendering of the area, derived from the high-resolution DEM. Essentially, this indicates the "ground truth" topography.

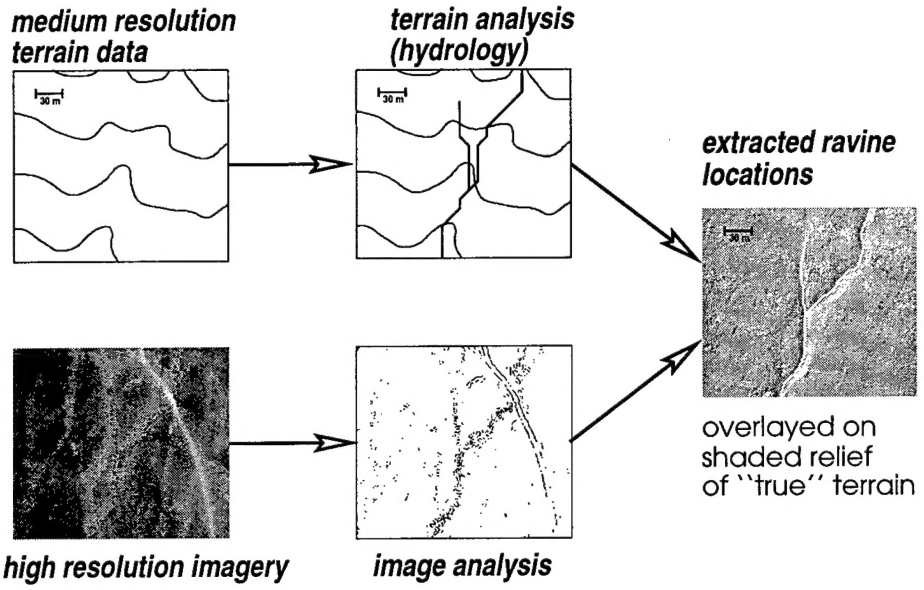

Figure 2: Combining terrain analysis and computer vision for ravine extraction.

4 Background

4.1 Hydrological Analysis for Terrain Analysis

The earliest ideas on using DEM data to find ravines were based on using local surface properties to look for a part of the topographic surface that is locally concave-upward, and mark this position as a valley or ravine, presuming that it is where surface water runoff is likely to be concentrated (e.g., [6, 7, 8]). Differential properties of the height field can achieve a similar effect [9]. Many researchers (e.g., [10, 11]) have used a method that is more physically justifiable in nature. In this method, a direction is assigned to each cell of the DEM, corresponding to the direction that water would flow out of that cell. This direction is that of steepest decent (i.e., one of the 8 compass directions that corresponds to the steepest downhill slope from that cell). Given this "direction matrix," the total number of cells of the DEM that contribute drainage through each cell is calculated. Those cells that accumulate drainage above a certain threshold are considered part of the drainage network.

4.2 Active Contours for Image Analysis

Active contours (often called *snakes*) are a powerful tool for finding long curving linear structures in images [12]. Snakes are introduced as energy-minimizing splines, whose energy is a weighted sum of internal and external energies. There are two different internal energies that may be weighted in order to force a snake to act more like a membrane or string, in the sense of it resisting stretching, or more like a thin-plate or rod, in that it resists bending [13]. The external energy equation is a function of the image on which it is acting. This equation can be specified to favor various image properties, such as edges and lines. Snakes bring to bear a high-level, global knowledge across the entire curve, instead of relying solely on local, low-level knowledge [12, 14]. In recent years, much research has been directed at various aspects of snakes, including initialization (e.g., [15, 16]), different underlying representation of snakes (e.g., [14, 17]), formulation of energy functions (e.g., [18, 19]), imposing constraints (e.g., [20, 21]), and the method of solution (e.g., [17, 22]).

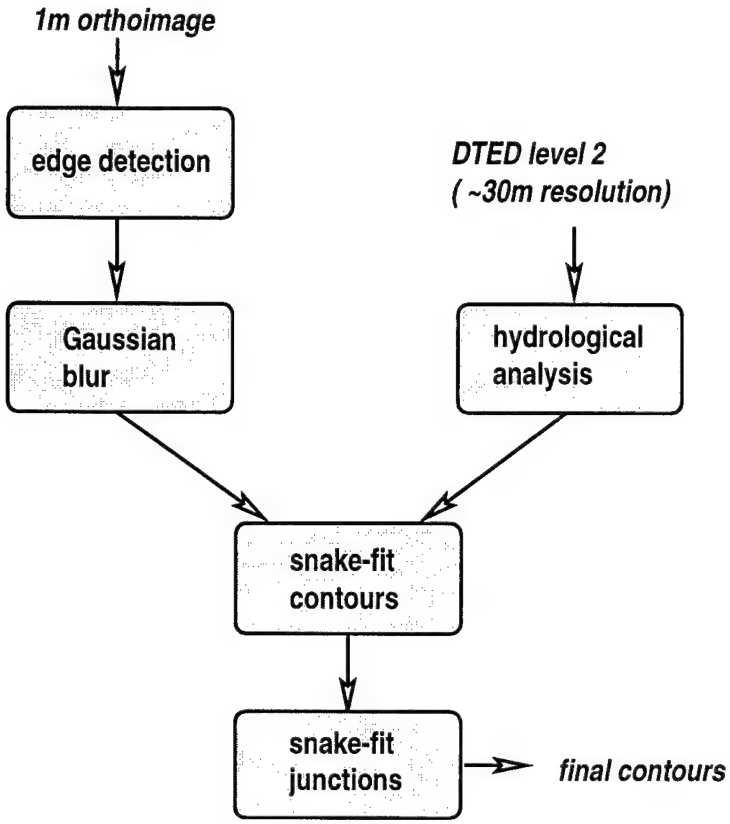

Figure 3: Overview of ravine extraction process.

5 Ravine Extraction

Our method uses a hydrological analysis to infer likely ravine locations. This information is used to initialize the snaking process. The external energy function is based on standard edge detection methods applied to an aerial image covering the same terrain. The refinement of contour location using the snaking process proceeds in two steps. The first adjusts individual segments of the tree of drainage patterns to best fit the imagery, subject to the contour smoothing criteria. The second step adjusts the junctions connecting multiple contour segments. (See Figure 3.)

5.1 Finding Drainage Features

Hydrological analysis was done using Arc/Info functions `flowdirection`, `flowaccumulation`, `con`, and `streamline`, which implement the steepest descent approach. DTED level 2 elevation source data was used. This is represented in a geographic (latitude/longitude) coordinate system, with a post spacing of 1 arc-second in both latitude and longitude. We used the slightly unconventional approach of doing the hydrological analysis in this spherical coordinate system to avoid the interpolation artifacts that would have been generated by reprojecting the geographic coordinates into a planar coordinate system. Instead, reprojection to a UTM coordinate system was done after the drainage patterns were found.

Figure 4 shows the NIMA ITD drainage features for a portion of the Range 400 area, overlayed onto an aerial image of the same region. Only one feature is present in this area and it is mislocated by as much as 40m. Figure 5 shows the drainage features for the same area, determined using the hydrological analysis.

Figure 4: ITD drainage features in a portion of Range 400.

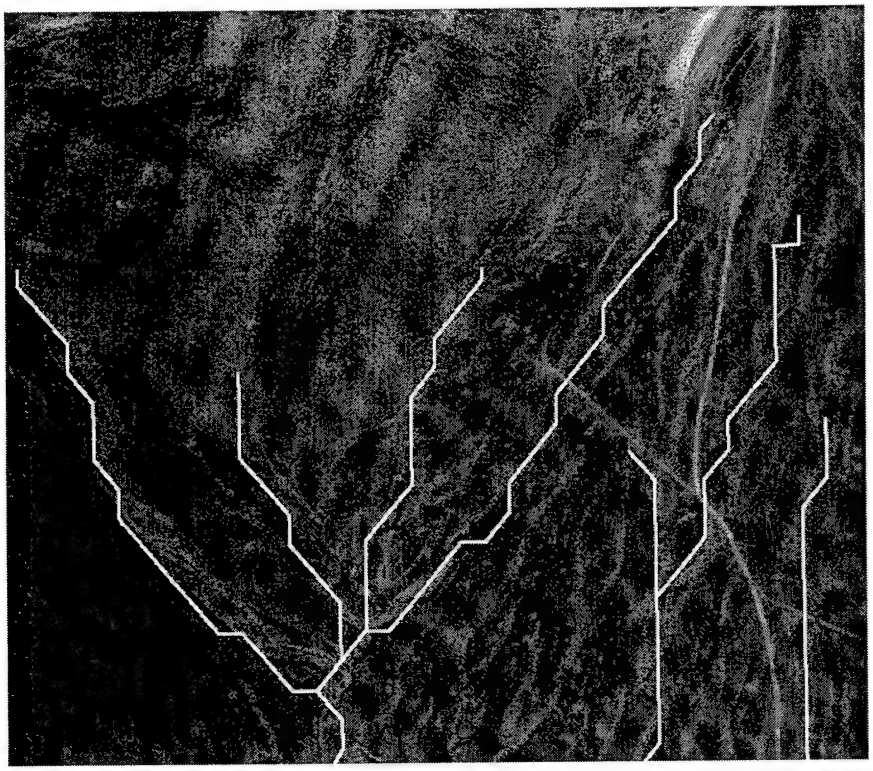

Figure 5: Drainage features for the same regions as shown in Figure 4, determined using hydrological analysis.

Many more relevant features are included. Locations are still incorrect, however, which is not surprising given the limited resolution of the source data.

5.2 Refining Drainage Features Using Aerial Imagery

A single aerial image, georeferenced to the elevation data on which the hydrological analysis is based, can be used to refine the location of drainage patterns to precisions on the order of the resolution of the image. Since high resolution imagery is much more likely to be available for a given area than is high resolution elevation data, this can greatly improve the fidelity of a terrain database.

While we can guess at the locations of ravines in images, such as those shown in Figure 4, the visual signature of ravines is easily confused with other commonly occurring terrain and cultural features. This ambiguity can be significantly reduced if we use a top-down approach that uses the results of hydrological analysis as a starting point for searching for ravines in the aerial imagery. Such an approach is easily implemented by using the results of the hydrological analysis as the starting estimate for a snaking computation. Snakes have the computational property that they will modify this estimate only in ways that make it better conform to the imagery.

The detailed appearance of ravines varies greatly, depending on local topography, soil type, and vegetation. As a result, standard contour extraction methods from computer vision will not work. Instead, we need a method for finding linear patterns that vary in some visual property, without knowing the details of the variation. Using edge density has proven to be effective in implementing this criteria. Figures 6–12 show an example. Figure 6 is a 1m orthoimage of the same area shown in Figures 4 and 5. Figure 7 shows the output of a Canny edge detector applied to this orthoimage. Automated methods for choosing the threshold and size parameters of the Canny operator are described in [23].

Snaking requires a potential function with a spatial extent at least as big as the likely uncertainty in initial contour location. We do this by applying a Gaussian blur to a binary representation of the edge image, using a standard deviation on the order of the resolution of the elevation image used as the basis of the hydrological analysis (Figure 8). As iterations of the snaking process proceed, the potential function is modified by reducing the amount of blur applied to the edge image [23]. This has the effect of increasing the spatial localization of the final estimates.

Figure 9 shows the final results of this process, indicating how much refinement has occurred over an analysis based only on the DTED level 2 elevation data (Figure 5). In Figure 10, these features have been overlayed on top of the original aerial image. The availability of accurate, high-resolution elevation data for Range 400 lets us compare the results with the actual terrain. Figure 11 shows the final estimated ravine locations overlayed on a shaded relief rendering of the terrain, based on the 1m DEM. Over most of the area, ravine centerlines are found to within a few meters of the correct location. It is important to note that the 1m elevation data are used only to validate results. The actual data extraction is based on DTED level 2 elevation data (with approximately 30m post spacing and well above 30m resolvable detail) and a single, 1m resolution aerial image. Figure 12 shows the final ravine features extracted over the whole of the Range 400 area, again overlayed onto a shaded relief rendering of the high-resolution DEM.

Figures 13 and 14 give an indication of the improvements that can be obtained from this approach on real terrain simulation applications. Figure 13 shows a view generated from the CCTT Primary Two database from a vantage point in the Range 400 area. The ravine that is shown was entered into the database using ITD features. In Figure 14, the database has been modified by removing ITD drainage features and replacing them with the features shown in Figure 12. The improvement in realism is immediately apparent. (The ravines remain standard width in order to satisfy CCTT SAF (Semi-Automated Forces) constraints.)

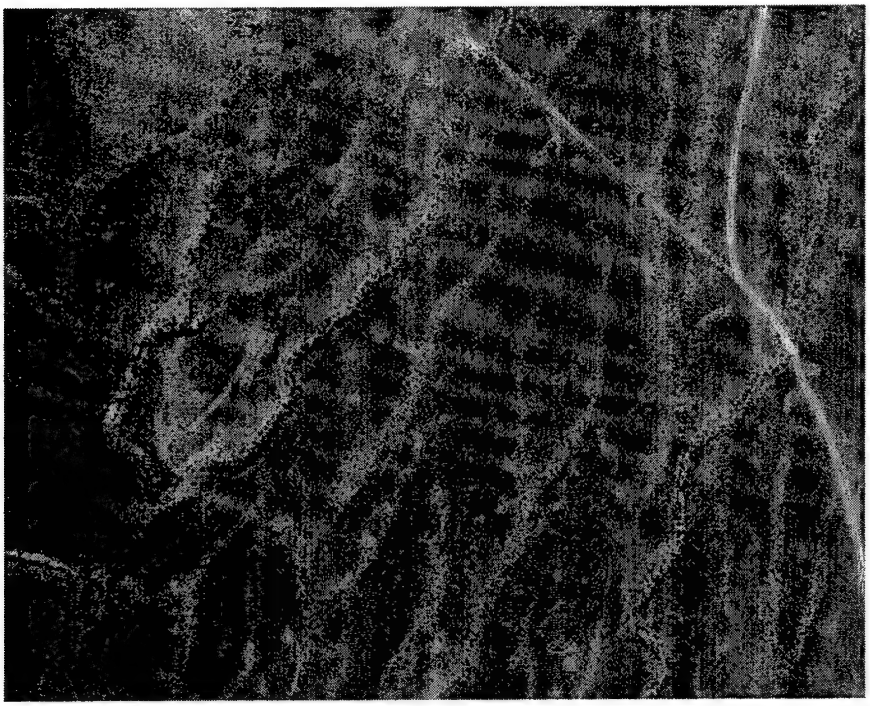

Figure 6: Aerial image.

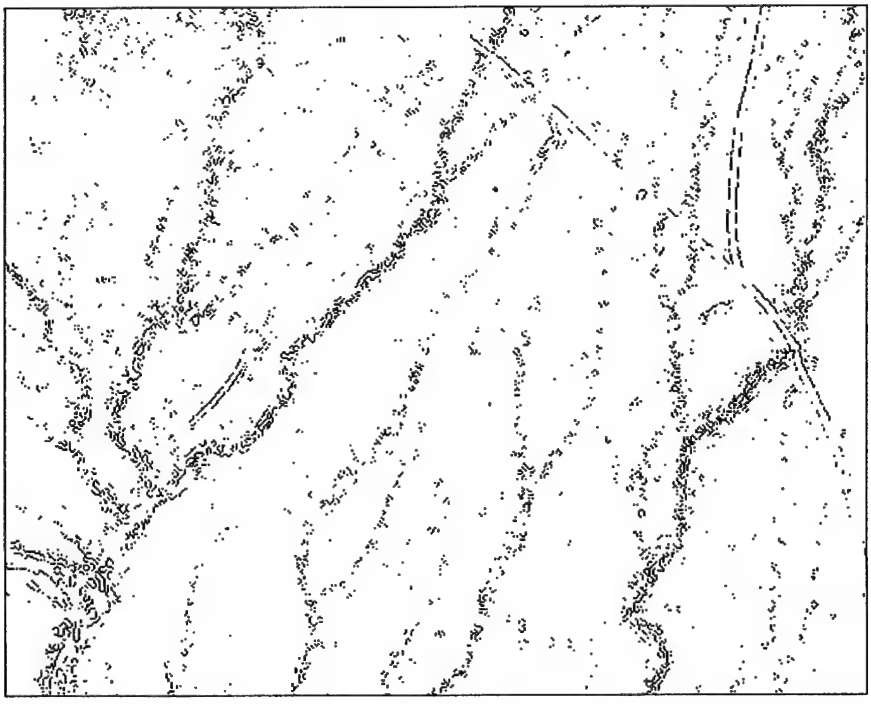

Figure 7: Edges derived from Figure 6.

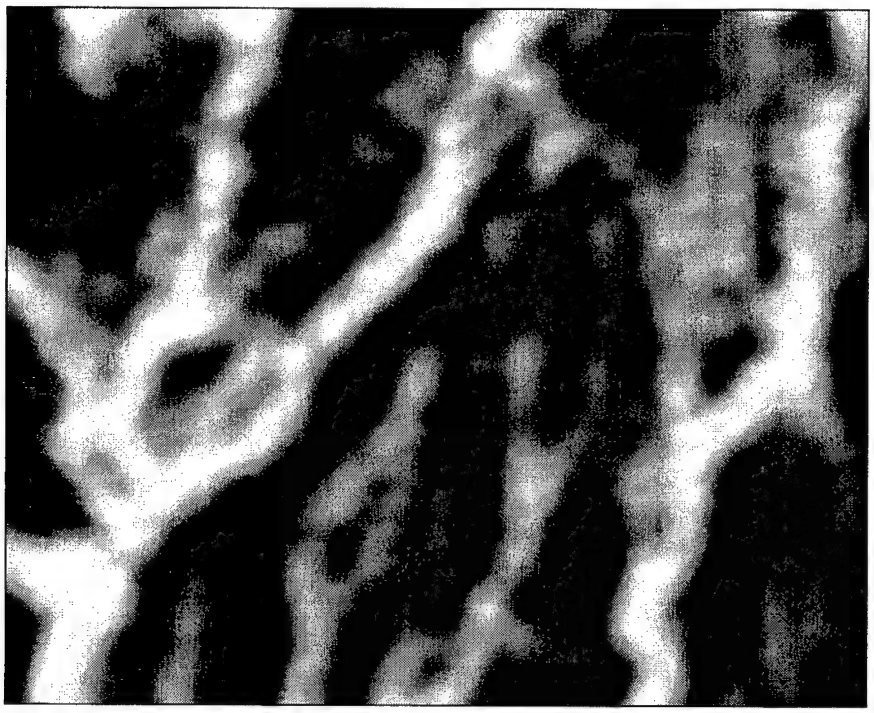

Figure 8: Potential function derived from edges shown in Figure 7.

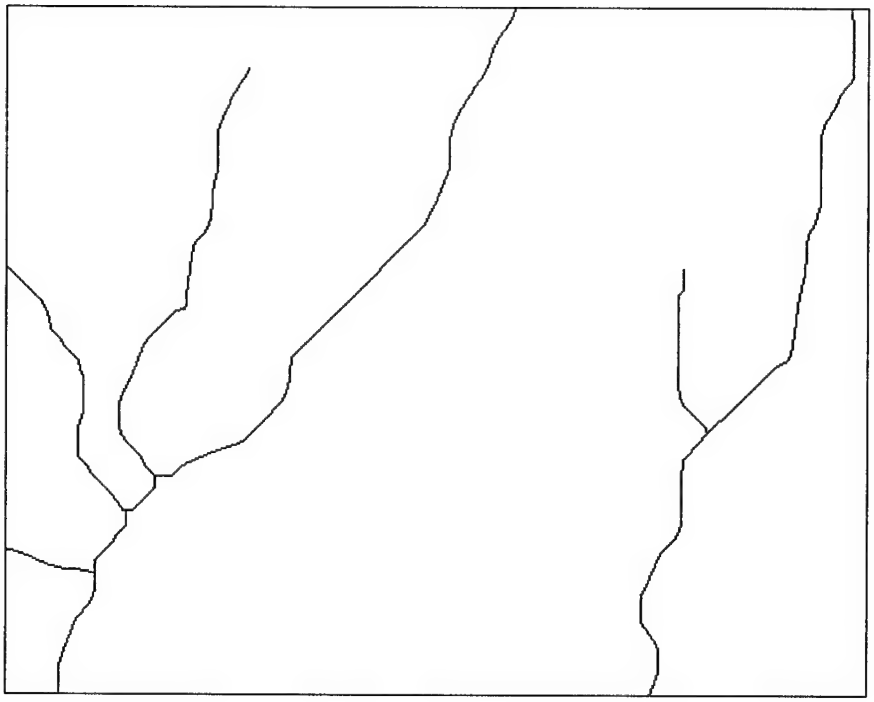

Figure 9: Final features.

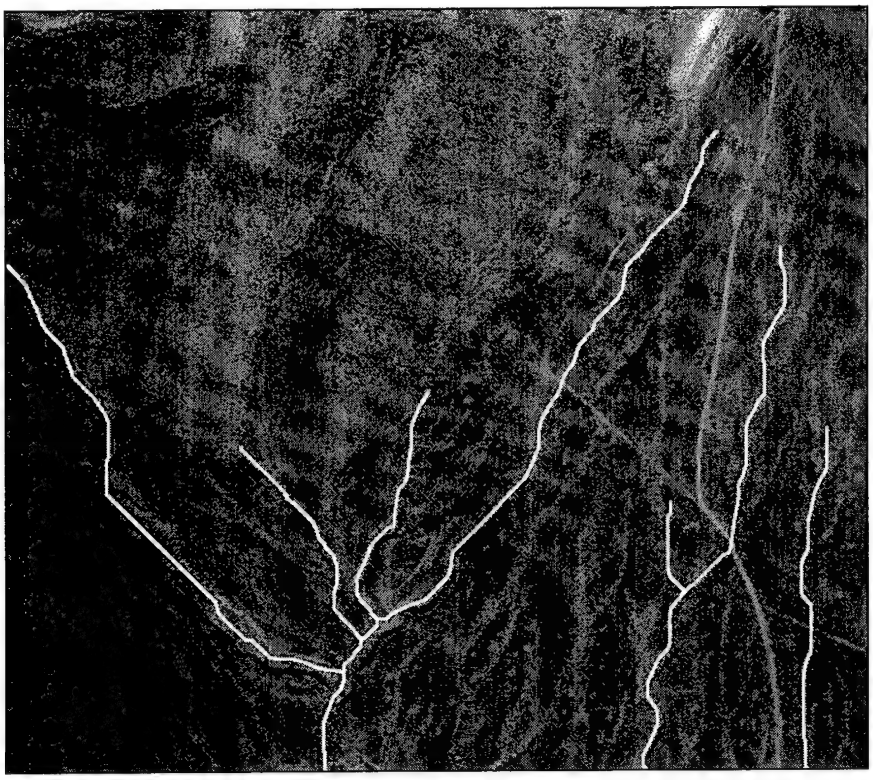

Figure 10: Final features, overlayed onto aerial image.

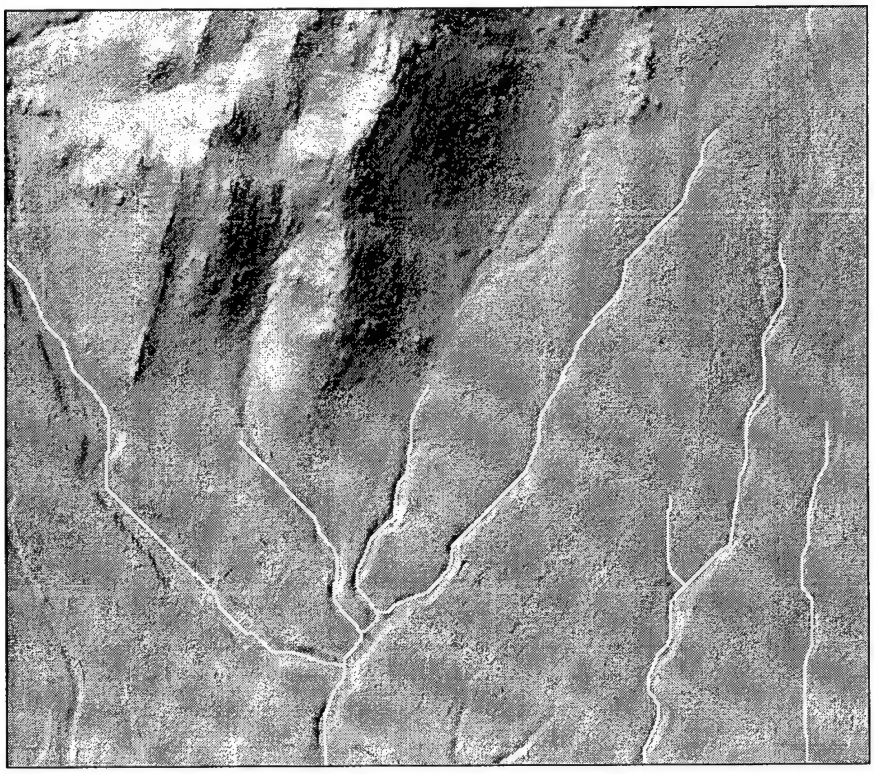

Figure 11: Final features, overlayed onto shaded relief generated from 1m elevation data.

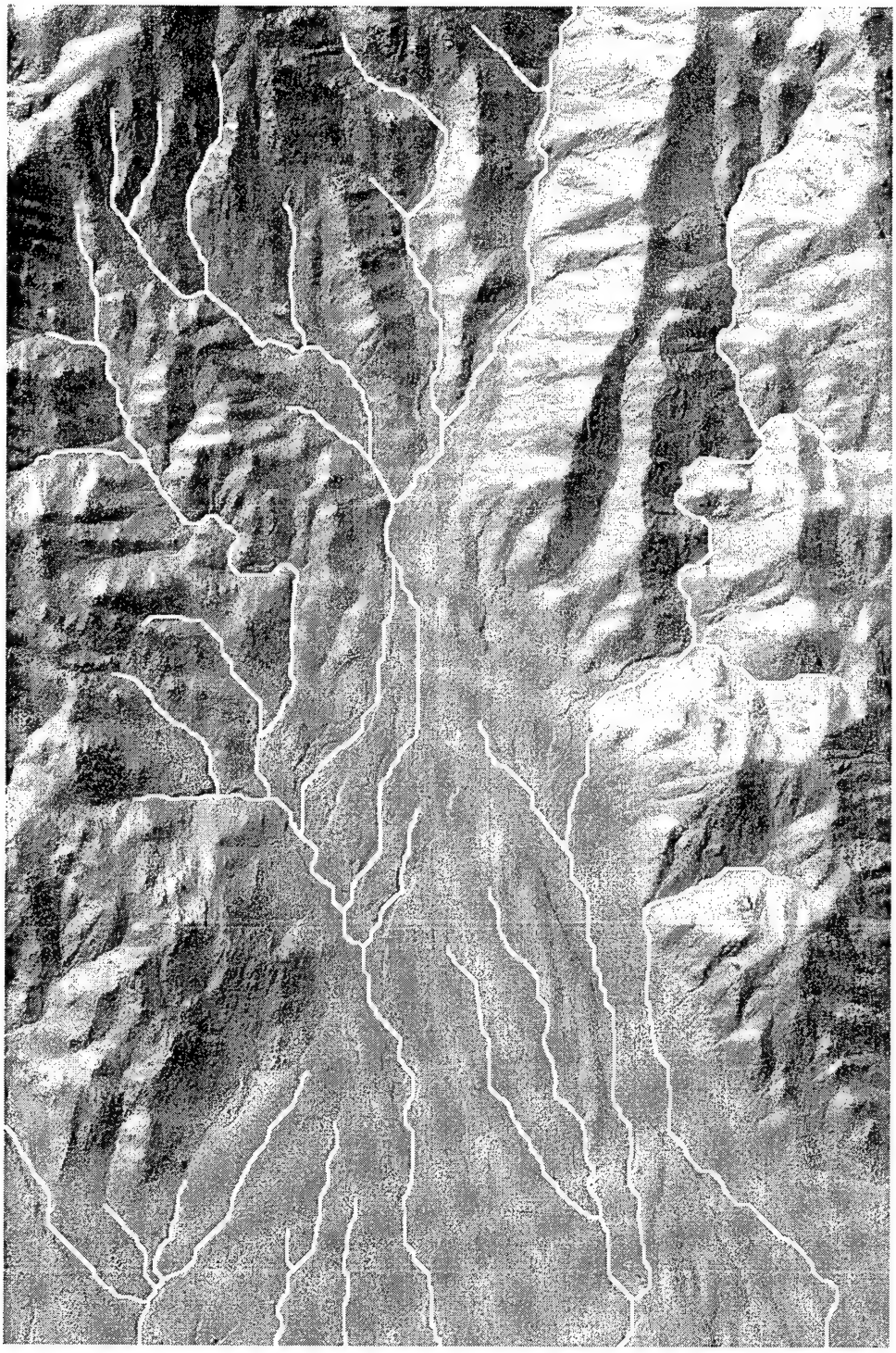

Figure 12: Final features – full Range 400, overlayed onto shaded relief.

Figure 13: CCTT database with ITD-based drainage features.

Figure 14: CCTT database with improved ravine features.

5.3 Comparison with Other Analyses of Range 400

Richbourg [4] conducted a study on the same Range 400 area as was used for demonstration in this report, with the intention of developing an automated terrain analysis tool to help with mission planning. Part of this study was to determine the best defensive positions in the area and the best offensive routes by both armor and infantry to overtake those positions. These were determined by analysis of the high-quality 1m data of the area, and compared against visual analysis of the area and prior defensive positions and offensive routes of the soldiers training in the area. Figures 15 and 16 are hand-drawn replicas of Richbourg's Figures 8 and 6, respectively [4].

As part of planning the route for the armor, an analysis on the terrain was performed in order to determine where armor could physically travel. Those parts of the "flats" of Range 400 that were deemed inaccessible for tanks (because of high forward or side slopes, or ground clearance requirements) are marked in black in Figure 15. Not surprisingly, many of these sections correspond to banks of washes.

Figure 16 shows the offensive infantry routes chosen by Richbourg's analysis of the 1m elevation data. These routes correspond to minimum cumulative visibility (from the defensive positions) approaches to the defensive positions. He notes the close correspondence between the concealed routes and the washes. He also notes that these routes correspond very closely to those encouraged by the trainers and used by the training attacking infantry.

Figure 17 shows an overview of the wash locations determined by the method discussed in this report, augmented with additional tools for automated parameter setting [23]. As can be seen, almost the entire route determined by Richbourg as optimal for the infantry movement is designated as a wash. Notice that most of the sections of Range 400 designated as impassable for armor by Richbourg also correspond to wash locations. Note that there are more determined wash locations than spots that are a hindrance to armor mobility, which is sensible considering that not all parts of all washes will have the steep sides that confine tanks. Note also that some of these washes appear to be offset from the spots that hinder armor, which is also sensible as it is the sides of the washes that hinder armor, and different parts of the washes (i.e. sides and middles) are found using the process based on elevation and image data.

Richbourg ran a comparison on the effects of using different resolution elevation data on planning the routes with his automated analysis of the terrain by subsampling the 1m elevation data to 2m, 3m, 5m, 10m, 15m, and 30m. He found that 2m and 3m post spacings would work well for the analysis, with analysis of the 3m elevation data suggesting routes that had only 6 percent more cumulative exposure in them than the routes planned from analyzing the 1m elevation data. However, analyzing data with lower resolution than these produced unacceptable paths, as analysis of even 15m data (twice what is currently available in DTED data) produced suggested routes with nearly double the cumulative exposure to the offensive infantry.

As can be seen, results comparable to those obtained by Richbourg on elevation data with post spacings of a few meters also can be found using DTED level 2 elevation data (with a nominal post spacing of approximately 30m, but with a true resolution far worse than what would be obtained subsampling Richbourg's data every 30 meters) augmented with a single higher resolution orthoimage.

Figure 15: Location of sections of Range 400 that were deemed by Richbourg as untraversable by armor are shown in black.

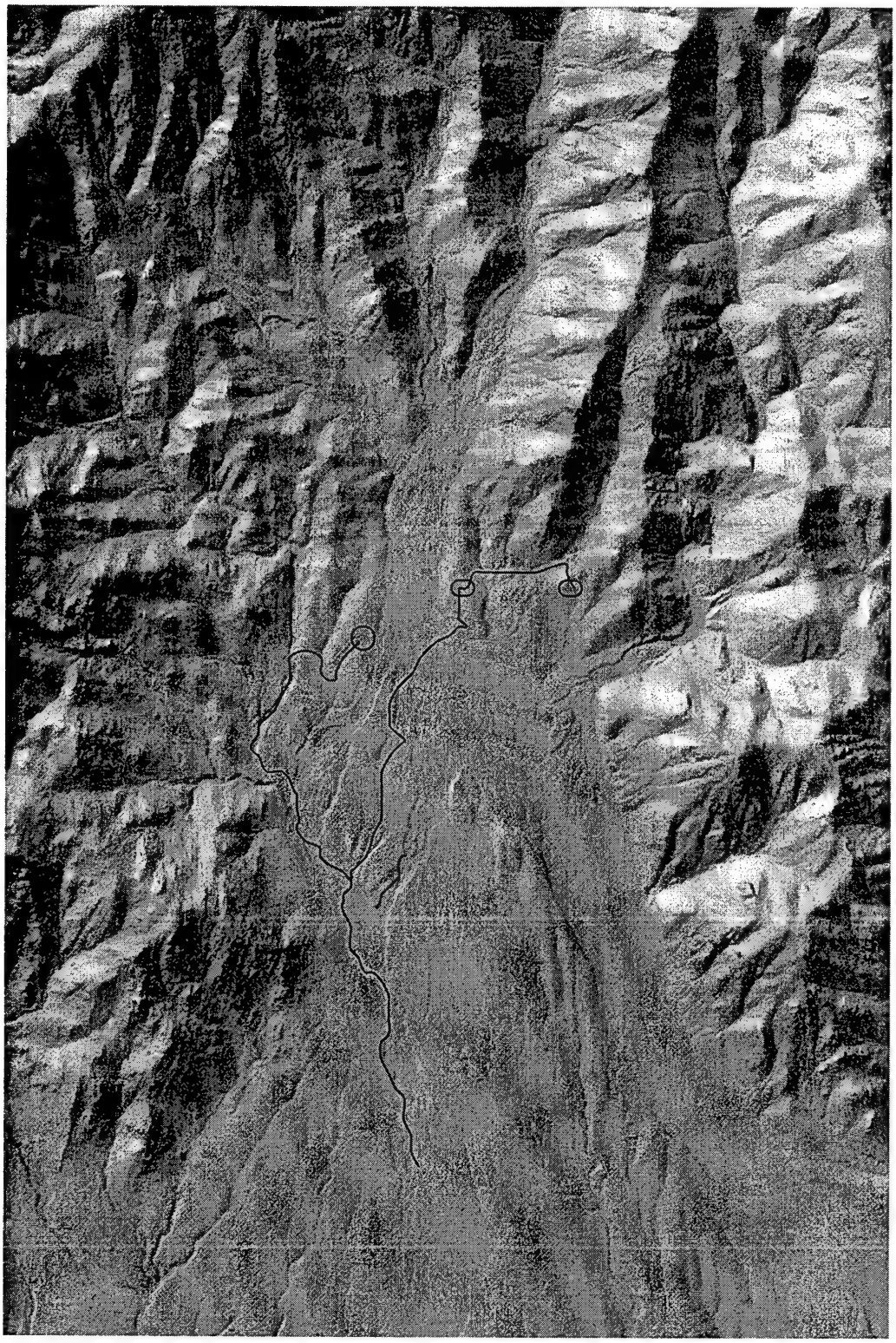

Figure 16: Marked in black are the routes determined by Richbourg from analysis of the high-quality 1m elevation data to be minimum visibility approaches to the defensive positions (marked by black ellipses).

Figure 17: Marked in black are the locations of washes as determined by analysis of 30m elevation data and 1m orthoimage.

6 Determine the Width of Ravines

The method just described is effective at finding the centerlines of ravines, but it tells nothing about the cross-section of the ravine. A complete cross-section analysis would require high-resolution 3–D photogrammetry, which in turn depends on the availability of very precisely controlled and calibrated stereo imagery. A straightforward extension of the snaking procedure outlined above, however, can be used to find the location of the two sidewalls of a ravine using only a single aerial image.

If ravines had near constant width, *ribbon snakes* [24, 16, 25] could be used. Since width is highly variable, a different approach is needed. Our method starts by first finding the location of ravine centerlines. This is used to initialize a second snaking process. Each centerline is split into two contours. These contours are optimized using a second potential function that is the gradient magnitude of the first potential function (which in turn was based on edges in the image). The effect is to create a new potential function with local maxima where the edge density in the image is changing most rapidly. The dot product of the gradient direction of the first potential function and the normal of the initial contours is used to insure that one contour is drawn to each side of the ravine.

Figures 18–23 show the results of applying this approach. Figures 18 and 19 are the same image and initial potential function as shown in Figures 6 and 8. Figure 20 shows the gradient magnitude of Figure 8. Figures 21-23 show the final ravine sidewall locations, overlayed onto the original aerial image in Figure 22 and onto the shaded relief rendering of the 1m elevation data in Figure 23. Again, the high-resolution elevation data is used only to validate the results, it was not part of the feature extraction process. Figure 24 shows the final ravine sidewall features extracted over the whole of the Range 400 area, overlayed onto a shaded relief rendering of the high-resolution DEM. Figure 25 gives an indication of just how accurate these extracted features are. The figure was produced by draping the aerial image and the ravine sidewall extracted from the lower-resolution elevation data onto the high resolution DEM. It is likely that hand processing would not have produced results more accurate than this automated process.

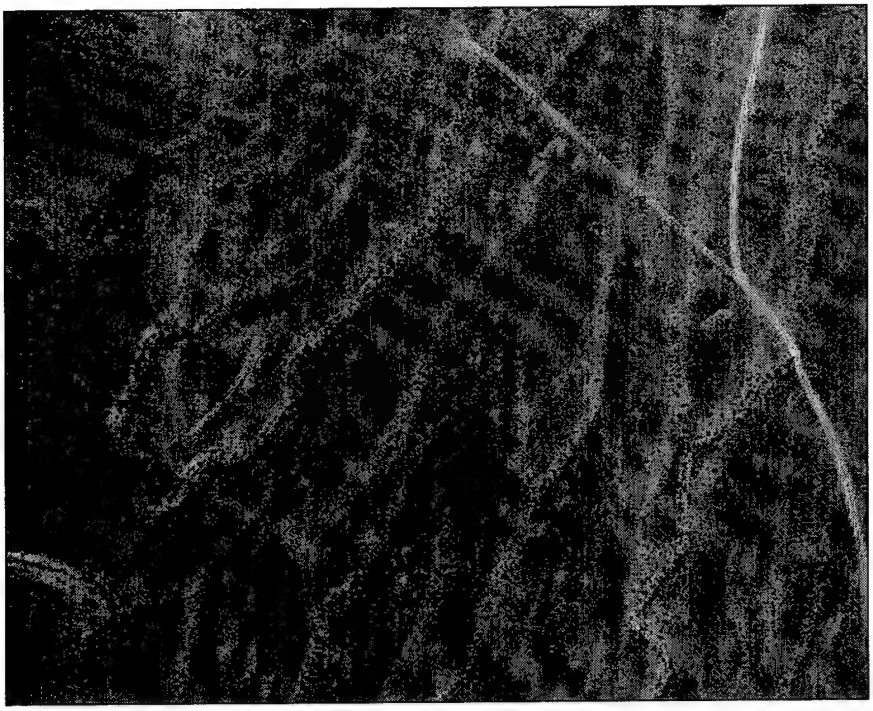

Figure 18: Aerial image.

Figure 19: Potential function.

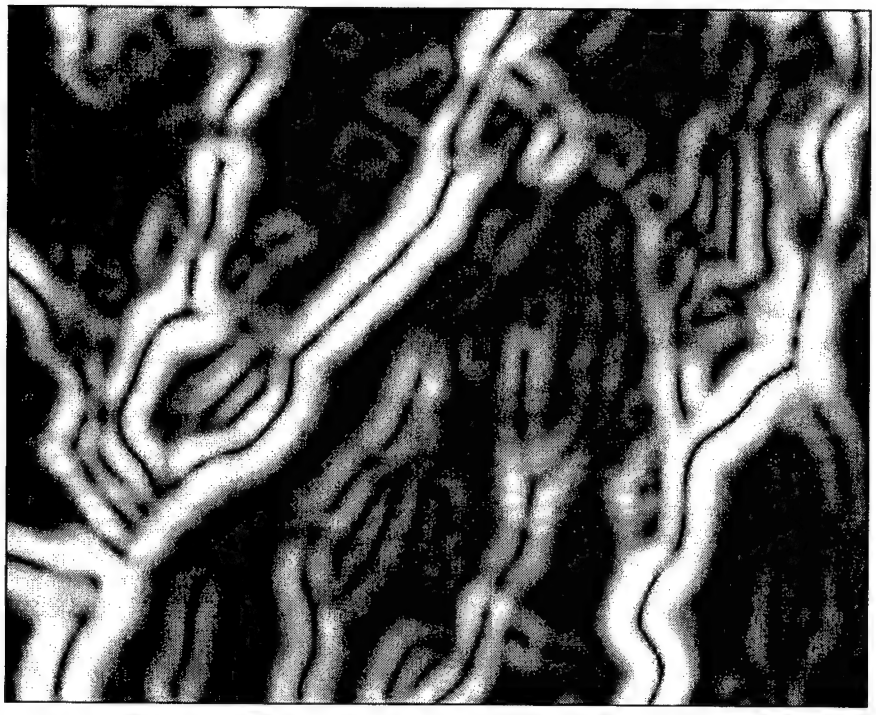

Figure 20: Gradient of potential function.

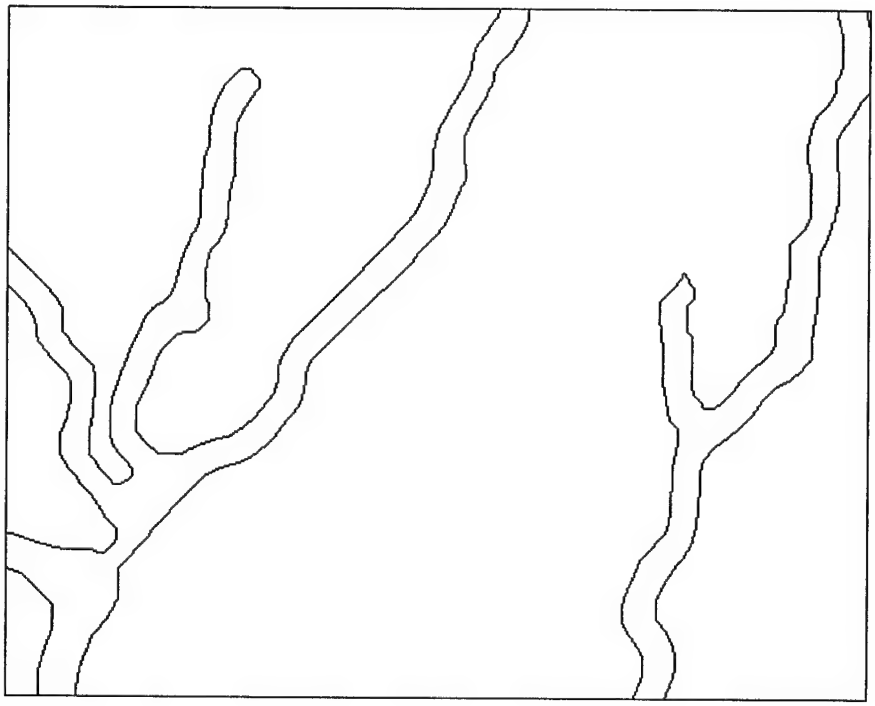

Figure 21: Extracted ravine sides.

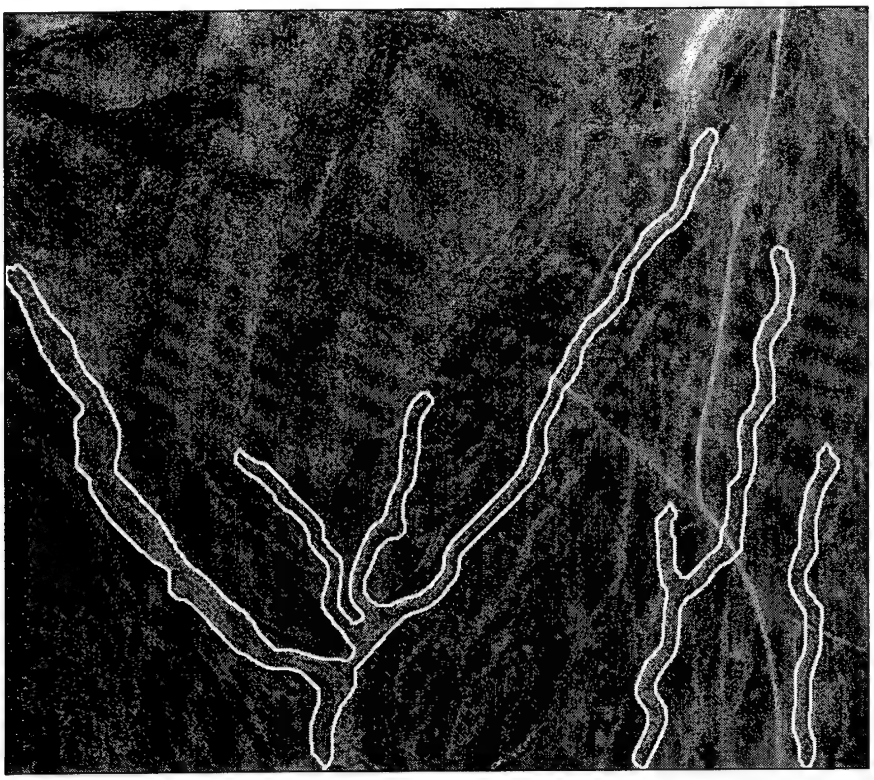

Figure 22: Extracted ravine sides, overlayed onto aerial image.

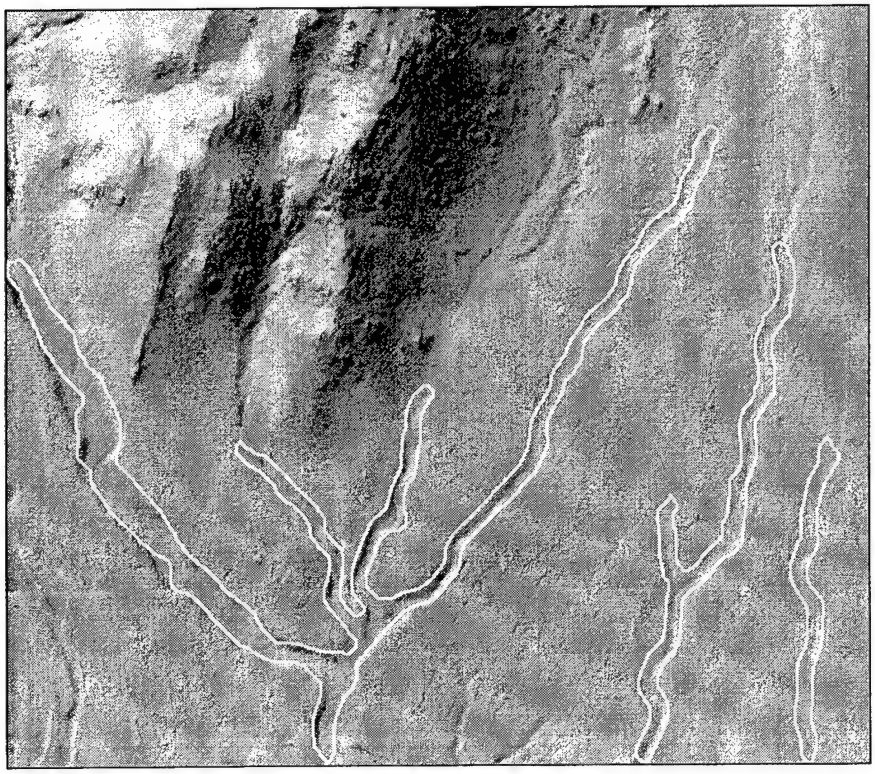

Figure 23: Extracted ravine sides, overlayed onto shaded relief.

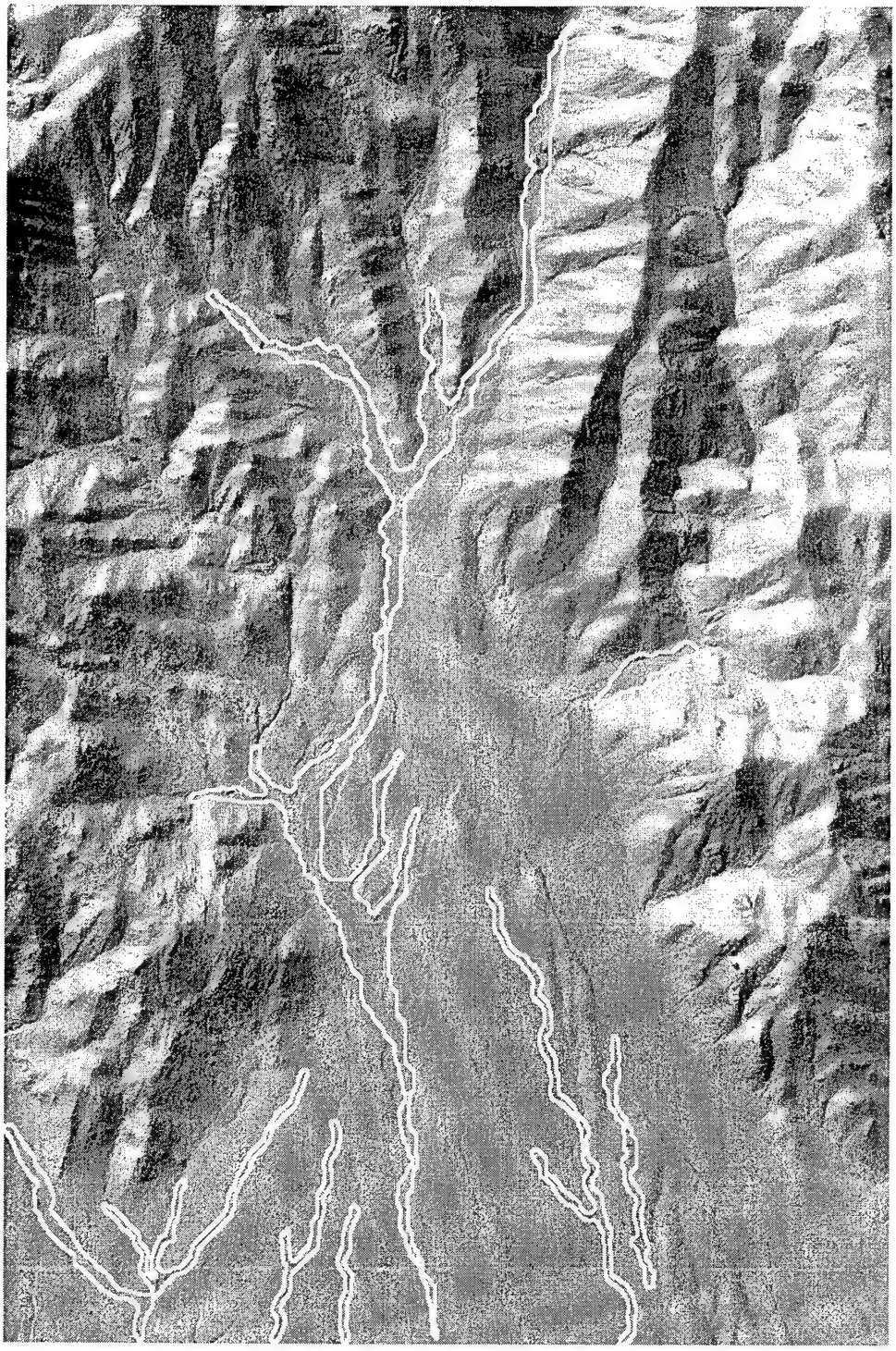

Figure 24: Extracted ravine sides – full Range 400, overlayed onto shaded relief.

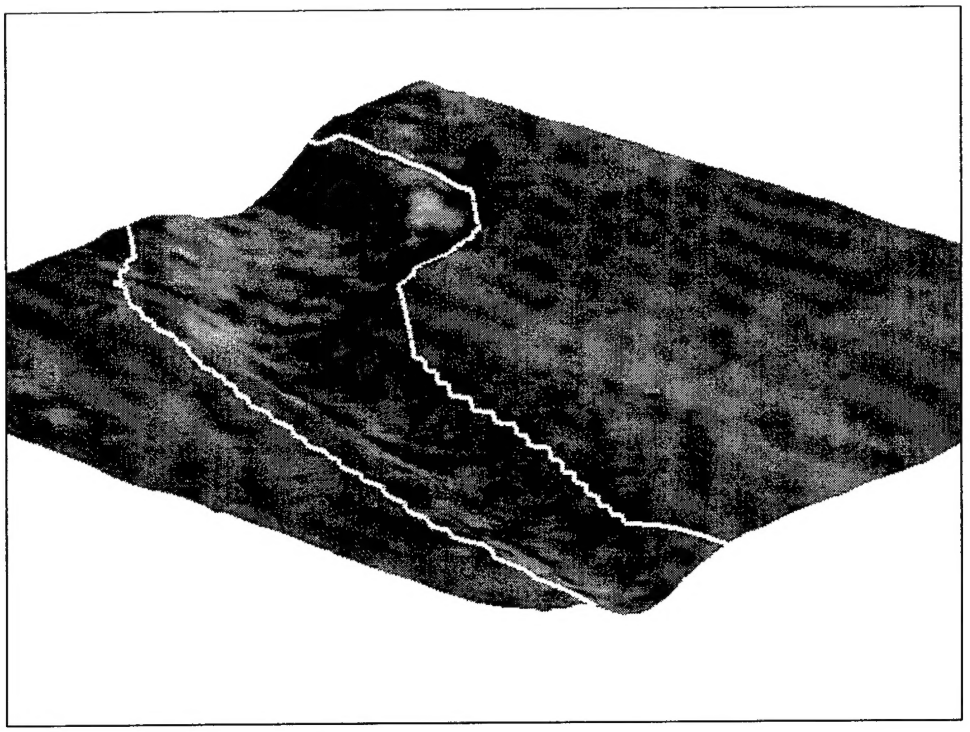

Figure 25: Extracted ravine sides rendered onto high-resolution DEM.

7 Using Active Contours to Refine Existing Features

The method described above uses snakes (active contours) to refine the location of linear features first estimated from medium resolution elevation data using a hydrological analysis. The computer vision component of this approach also can be used to improve the accuracy of features already present in a database. Figures 26 and 27 give an example. Figure 26 shows an ITD drainage feature in a canyon section of the Range 400 area, overlayed onto an aerial image of the same region. Clearly, the feature is not accurately located, with errors of as much as 65m being present. Figure 27 shows the results of using the ITD feature as an initial estimate in the snaking process and then refining this estimate using the imagery. The result is far better localization of the features.

More generally, tools such as this will become increasingly important as more and more visual simulations use image mapping techniques rather than stereotypical texture mapping. When image mapping is used, it is critical that the geometry and functional behavior of the terrain model match the image that is rendered. The same top-down, model-driven image analysis techniques used for ravine extraction can aid in consistent modeling of a wide range of features.

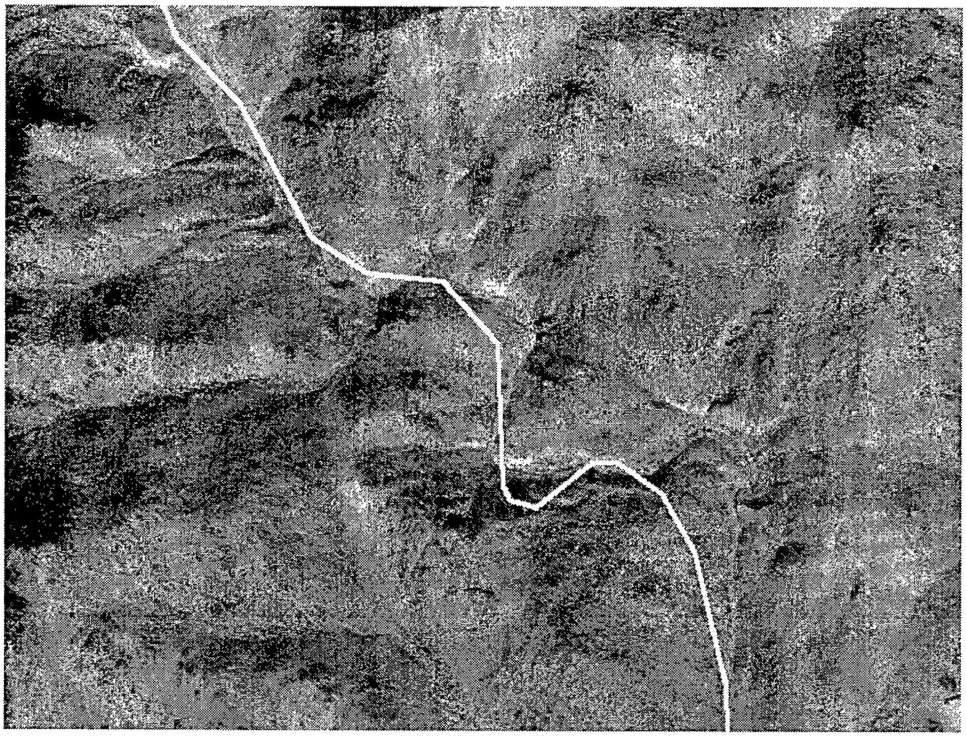

Figure 26: ITD drainage feature.

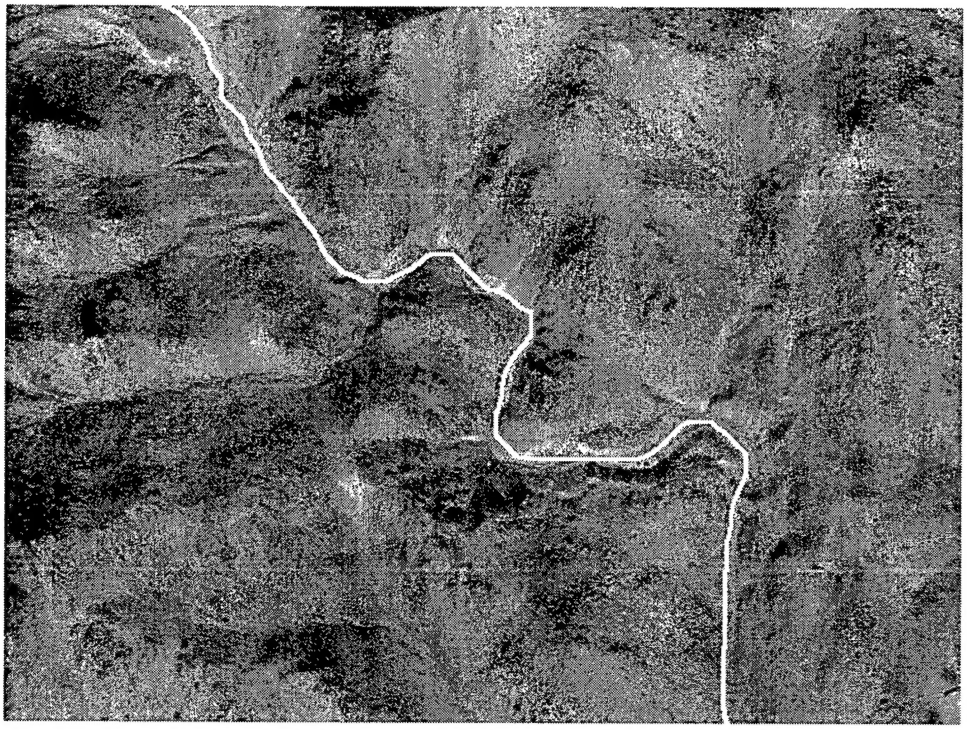

Figure 27: Refined ITD drainage feature.

References

[1] Thompson, W. B., and T. C. Henderson, "IU at the University of Utah: Extraction of micro-terrain features," in *Proceedings DARPA Image Understanding Workshop*, May 1997.

[2] Pope, C. N., M. Vuong, R. G. Moore, and S. S. Cowser, "A whole new CCTT world," *Military Simulation and Training*, no. 5, 1995.

[3] Richbourg, R., C. Ray, and L. L. Campbell, "Terrain analysis from visibility metrics," in *Conference on Integrating photogrammetric techniques with scene analysis and machine vision II, (SPIE Proceeding Volume 2486-2)*, (Orlando, FL), April 1995.

[4] Richbourg, R., and W. K. Olson, "A hybrid expert system that combines technologies to address the problem of military terrain analysis," in *Expert Systems and Applications*, 1996.

[5] Thoenen, G. W., and W. B. Thompson, "Extraction of micro-terrain ravines using image understanding constrained by topographic context," in *Proceedings DARPA Image Understanding Workshop*, May 1997.

[6] Peucker, T. K., and D. H. Douglas, "Detection of surface-specific points by local parallel processing of discrete terrain elevation data," *Computer Graphics and Image Processing*, vol. 4, pp. 375–387, 1975.

[7] Chorowicz, J., J. Kim, S. Manoussis, J. P. Rudant, P. Foin, and I. Veillet, "A new technique for recognition of geological and geomorphological patterns in digital terrain models," *Remote Sensing of Environment*, vol. 29, pp. 229–239, 1989.

[8] Tribe, A., "Automated recognition of valley lines and drainage networks from grid digital elevation models: A review and a new method," *Journal of Hydrology*, vol. 139, pp. 263–293, 1992.

[9] Henderson, T. C., S. Morris, and C. Sanders, "Ridge and ravine detection in digital images," in *Proceedings DARPA Image Understanding Workshop*, May 1997.

[10] Mark, D. M., "Automated detection of drainage networks from digital elevation models," in *Auto-Carto VI: Proceedings Sixth International Symposium on Computer Assisted Cartography*, pp. 288–298, 1983.

[11] Jenson, S. K., and J. O. Domingue, "Extracting topographic structure from digital elevation data for geographic information system analysis," *Photogrammetric Engineering and Remote Sensing*, vol. 54, no. 11, pp. 1593–1600, 1988.

[12] Kass, M., A. Witkin, and D. Terzopoulos, "Snakes: Active contour models," *International Journal of Computer Vision*, pp. 321–331, 1988.

[13] F. Leymarie and M. D. Levine, "Tracking deformable objects in the plane using an active contour model," *IEEE Trans. on Pattern Analysis and Machine Intelligence*, vol. 15, no. 6, pp. 617–634, 1993.

[14] Menet, S., P. Saint-Marc, and G. Medioni, "Active contour models: Overview, implementation, and applications," in *IEEE International Conference on Systems, Man and Cybernetics*, (Los Angeles, CA), pp. 194–199, 1990.

[15] Berger, M.-O., and R. Mohr, "Towards autonomy in active contour models," in *10th International Conference on Pattern Recognition*, (Piscataway, NJ), pp. 847–851, 1990.

[16] Neuenschwander, W., P. Fua, G. Szekely, and O. Kubler, "Initializing snakes," in *Proceedings IEEE Conference on Computer Vision and Pattern Recognition*, (Seattle, WA), pp. 658–663, June 1994.

[17] Wang, M., J. Evans, L. Hassebrook, and C. Knapp, "A multistage, optimal active contour model," *IEEE Transactions on Image Processing*, vol. 5, no. 11, pp. 1586–1591, 1996.

[18] P. Radeva, J. Serrat, and E. Marti, "Snakes for model-based segmentation," in *Fifth International Conference on Computer Vision*, (Cambridge, MA), pp. 816–821, 1995.

[19] Lai, K., and R. Chin, "On regularization, formulation and initilization of the active contour models (snakes)," in *Second Asian Conference on Computer Vision*, (Singapore), pp. 542–545, 1993.

[20] Neuenschwander, W., P. Fua, G. Szekely, and O. Kubler, "From ziplock snakes to velcro surfaces," in *Automatic Extraction of Man-made Objects from Aerial and Space Images*, pp. 105–114, Birkh auser Verlag, 1995.

[21] Fua, P., and C. Brechbuehler, "Imposing hard constraints on soft snakes," Tech Note 553, Artificial Intelligence Center, SRI International, October 1995.

[22] Amini, A., T. Weymouth, and R. Jain, "Using dynamic programming for solving variational problems in vision," *IEEE Trans. on Pattern Analysis and Machine Intelligence*, vol. 12, no. 9, pp. 855–867, 1990.

[23] Thoenen, G. W., "Extraction of micro-terrain ravines using hydrological analysis combined with active contours," Master's thesis, University of Utah, December 1998.

[24] Fua, P., and Y. Leclerc, "Model driven edge detection," *Machine Vision and Applications 3*, pp. 45–56, 1990.

[25] Davatzikos, C., and J. Prince, "Convexity analysis of active contour problems," in *Proceedings IEEE Conference on Computer Vision and Pattern Recognition*, pp. 674–679, 1996.